WATER VAPOR VERTICAL DISTRIBUTION DURING PERIHELION SEASON OF MARTIAN YEARS 34 AND 35 OBSERVED WITH NOMAD-SO.

A. Brines, *(adrianbm@iaa.es)*, **M. A. López-Valverde, A. Stolzenbach, A. Modak, B. Funke, F. G. Galindo, J.J. Lopez-Moreno,** *IAA/CSIC, Granada, Spain*, **S. Aoki,** *Japan Aerospace Exploration Agency (JAXA), Japan*, **G.L. Villanueva, G. Liuzzi,** *NASA Goddard Space Flight Center, USA*, *American University, Washington DC, USA*, **I.R. Thomas, J.T. Erwin, F. Daerden, L. Trompet, B. Ristic, A.C. Vandaele,** *Royal Belgian Institute for Space Aeronomy, Belgium*, **U. Grabowski,** *Karlsruhe Institute of Technology, Institute of Meteorology and Climate Research, Karlsruhe, Germany*, **F. Forget,** *Laboratoire de Météorologie Dynamique, IPSL, Paris, France*, **M.R. Patel,** *Open University, UK*, **G. Bellucci,** *Istituto di Astrofisica e Planetologia, Italy*.

Introduction

In the Martian atmosphere, water vapor is crucial in most of the chemical and radiative processes, playing a significant role in the planet's climate. Recent observations have proven that in the past, Mars was wetter than today, meaning that processes like the escape of water to the space have driven the planet to its current state. Also, previous works have pointed out how important is the vertical distribution of the water in the atmosphere for the evolution of the planet and for the understanding of the physical and chemical processes driving the water cycle [1]. However, despite its importance, there are many open debates, in particular those devoted to its vertical distribution.

Since April 2018, when Nadir and Occultation for MArs Discovery (NOMAD) onboard the ExoMars 2016 Trace Gas Orbiter (TGO) started its science phase, we are capable of sounding the Martian atmosphere with an unprecedented vertical resolution using the solar occultation technique.

Recent studies with the Atmospheric Chemistry Suite (ACS), also onboard TGO, and NOMAD revealed an enhancement of water vapor at high altitudes duirng dust events such as the Global Dust Storm during MY34 [2, 3, 4]. Other works focused on the hydrogen escape [5, 6] have suggested that the dust enhancement has a strong effect on the escape processes.

Here we present vertical profiles of water vapor from solar occultation observations by NOMAD, analyzing the water distribution and its seasonal and latitudinal variability during the first half of the perihelion season of two consecutive Martian Years (MY), allowing an extensive and direct comparison between MY34 and MY35.

NOMAD-SO measurements

NOMAD [7, 8] is an infrared spectrometer working in the spectral range between 0.2 to 4.3 μm. It has two IR spectral channels (SO and LNO) and one operating in the UV-visible spectral range (UVIS; 200-650 nm). The SO (Solar Occultation) channel covers the range between 2.3 and 4.3 μm (2320-4350 cm^{-1}) and uses an echelle grating with a density of $\sim$4 lines/mm and has a spectral resolution of $\lambda/\Delta\ \lambda \simeq 20000$. The sampling time of this channel is $\sim$1 s allowing a vertical sampling in the observations of $\sim$1 km. An Acousto-Optical Tunable Filter (AOTF) is used to select different spectral windows of a width of $\sim$30 cm^{-1} corresponding to the desired diffraction orders to be used during the observation. The AOTF quick change from one diffraction order to another allows to observe the atmosphere at a given altitude through 6 different spectral ranges within 1 second.

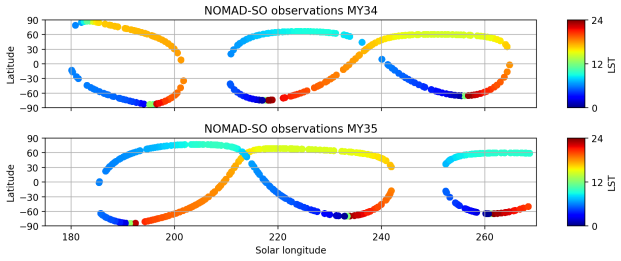

Figure 1: NOMAD observations analyzed during the selected period with SO diffraction orders 134 and 168. The observations during MY34 are shown in the top panel and during MY35 in the bottom panel. Color indicates the Local Solar Time.

For this study we have selected two subsets of measurements in MY34 and MY35 covering the same seasonal period between the solar longitudes $L_S = 180°$ and $L_S = 270°$, corresponding to the first half of the perihelion season. We have analyzed a total of 962 observations taken at the NOMAD-SO diffraction order 134 (3011 - 3035 cm^{-1}) and 168 (3775 - 3805 cm^{-1}) and its latitudinal coverage is shown in Figure 1.

Methodology

Here we use Level 1 SO data provided by the NOMAD calibration team that are processed with an in-house-develpoed software to evaluate and to correct for

residual bending in the continuum and for a remaining spectral shift [9]. To do so, we use the radiative transfer model KOPRA (Karlsruhe Optimized Radiative transfer Algorithm described in [10]) to generate a radiative forward model. The instrumental response of the AOTF and the Instrumental Line Shape (ILS) is included into the forward model using the latest calibration proposed by the NOMAD consortium and described in [5]. The reference atmosphere needed by the forward model is obtained from the Mars Global Climate Model developed at the Laboratoire de Météorologie Dynamique (LMD-MGCM) [11]. For each observation, a temperature and density profile was extracted from the model at the exact location and time of the occultation path at 50 km altitude. For the inversion of the vertical profiles, we use the Retrieval Control Program (RCP) developed at Institut für Meteoriologie und Klimaforschung (IMK) which incorporates the KOPRA forward model. After the inversion of each scan, we combine the retrieve profiles of the simultaneous scans of diffraction orders 134 and 168. Since the intensity of the water absorption lines in these two orders is noticeably different ($S_{134} \sim 10^{-21}$ and $S_{168} \sim 10^{-19}$ cm^{-1}/(molec·cm^{-2}) we decide to use the order 134 for the lower atmosphere and the order 168 for the upper atmosphere (above 60 km) to avoid the saturation of the absorption lines in the order 168 at low altitudes. Figure 2 shows the retrieved water vapor at one particular observation as an example. Also it shows the vertical resolution and the averaging kernels of the inversion.

With these profiles, we generate different sub-products to study different aspects of the Martian atmosphere.

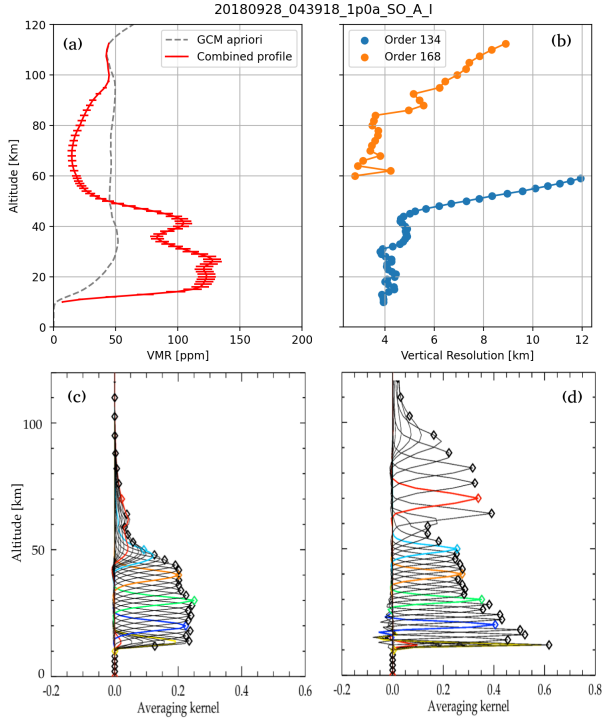

Figure 2: Performance of the retrieval of the data taken at the observation 20180928_043918_1p0a_SO_A_I. Panel (a) shows the retrieved water vapor, panel (b) shows the vertical resolution obtained for the order 134 (blue) and 168 (orange). Bottom panels (c) and (d) show the the averaging kernels of the retrievals for orders 134 (c) and 168 (d).

Results and discussion

Here we present detailed maps showing the vertical distribution of the water vapor abundance and an estimation of the saturation ratio (1). To do so, we use the expression for the saturation pressure over water ice (2) derived by [12].

$$S = \frac{\mu_{H_2O}}{\mu_{sat}} = \mu_{H_2O}\frac{P_{tot}}{P_{sat}} \tag{1}$$

$$P_{sat}(T) = \exp\left(9.550426 - \frac{5723.265}{T} + 3.53068 \cdot \ln(T) - 0.00728332T\right) \quad 110 < T < 273\text{K} \tag{2}$$

The strong activity Global Dust Storm took place during the MY34 at $L_S = 190^\circ - 205^\circ$. Figure 3 shows an intense peak of water vapor at that period, with abundances about 150 ppm reaching the upper mesosphere. This strong increase is not observed during the same period of MY35, where water vapor does not exceed abundances of 50 ppm above 50 km

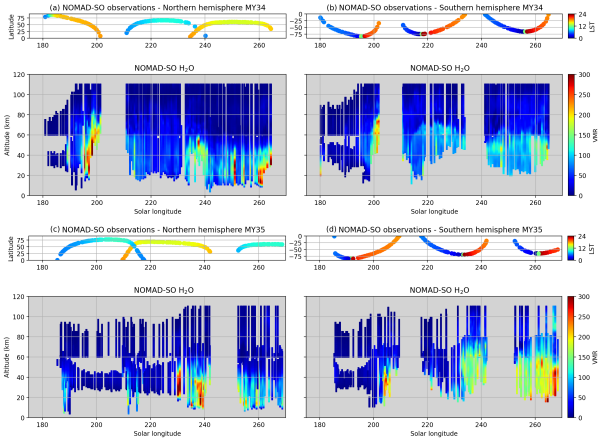

Figure 3: Vertical distribution of the retrieved water vapor. Panels (a) and (b) show the latitude of the of the observations (top) and the seasonal variation of the water vapor (bottom) at northern and southern hemispheres respectively for MY34. Panels (c) and (d) show the same information for MY35.

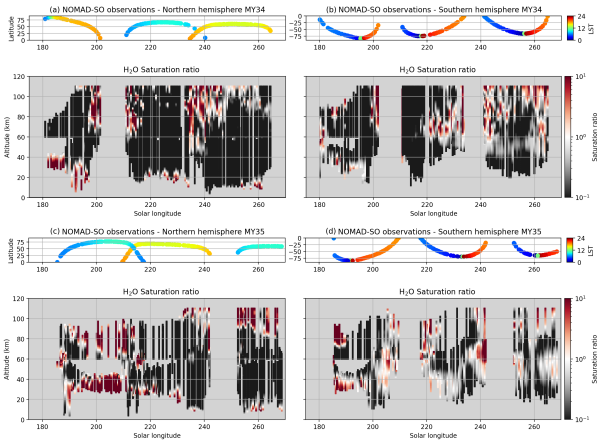

Figure 4: Same as Figure 3 but showing the estimated saturation ratio derived from the retrieved water vapor profiles.

revealing a strong contrast of the hygropause in dusty and non-dusty conditions. In Figure 4 we show the estimation for the saturation ratio calculated using LMD-MGCM temperatures. We observe multiple layers of supersaturation during both martian years at different altitude ranges and also several cases where water ice could be expected [13] in a supersaturated atmospheric environment. We will describe the H_2O distribution and saturation ratios in detail.

Comparison and validation

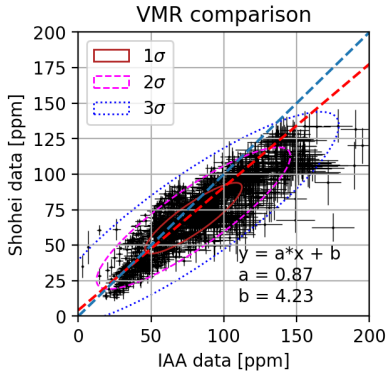

Figure 5: Comparison of the water vapor volume mixing ratio retrieved by IAA/CSIC and [14]. The blue dashed line shows the curve y = x and the red dashed line represents the linear fitting of the scattered data.

We have performed a first comparsion with other teams in the NOMAD consortium [14] for validation purposes and there is a global good agreement despite the different methodologies with very different approaches used for the retrievals, but with an averaged 13% larger H_2O in our retrievals. The comparison is shown in Figure 5.

Conclusions

We present water vapor vertical distributions during the first half of the Martian perihelion season from two consecutive Martian Years with a vertical sampling of 1 km and a mean vertical resolution of 4-6 km. We confirm a strong impact of the 2018 Global Dust Storm in the water vapor abundances during MY34 and a high contrast of the hygropause in dusty and non-dusty conditions. Also atmospheric supersaturation events with presence of water ice at mesospheric altitudes are reported.

Acknowledgments

The IAA/CSIC team acknowledges financial support from the State Agency for Research of the Spanish MCI through the Center of Excellence Severe Ochoa award (DEV-2017-0709) and funding by grant PGC2018-101836-B-100 (MCI/AEI/FEDER, EU). This project acknowledges funding by the Belgian Science Policy Office (BELLS), with the financial and contractual coordination by the ESAU Prod ex Office (PEA 4000103401,4000121493) as well as by UK Space Agency through grants ST/V002295/1, ST/V005332/1 and ST/S00145X/1 and Italian Space Agency through grant 2018-2-HHS.0. US investigators were supported by the National Aeronautics and Space Administration.

References

[1] L. Maltagliati, F. Montmessin, O. Korablev, A. Fedorova, F. Forget, A. Määttänen, F. Lefèvre, and J.-L. Bertaux, "Annual survey of water vapor vertical distribution and water–aerosol coupling in the martian atmosphere observed by SPICAM/MEx solar occultations," *Icarus*, vol. 223, no. 2, pp. 942–962, 2013.

[2] A. A. Fedorova, F. Montmessin, O. Korablev, M. Luginin, A. Trokhimovskiy, D. A. Belyaev, N. I. Ignatiev, F. Lefèvre, J. Alday, P. G. Irwin, *et al.*, "Stormy water on Mars: The distribution and saturation of atmospheric water during the dusty season," *Science*, vol. 367, no. 6475, pp. 297–300, 2020.

[3] S. Aoki, A. Vandaele, F. Daerden, G. Villanueva, G. Liuzzi, I. Thomas, J. Erwin, L. Trompet, S. Robert, L. Neary, *et al.*, "Water vapor vertical profiles on Mars in dust storms observed by

TGO/NOMAD," *Journal of Geophysical Research: Planets*, 2019.

[4] G. L. Villanueva, G. Liuzzi, M. M. Crismani, S. Aoki, A. C. Vandaele, F. Daerden, M. D. Smith, M. J. Mumma, E. W. Knutsen, L. Neary, *et al.*, "Water heavily fractionated as it ascends on Mars as revealed by ExoMars/NOMAD," *Science Advances*, vol. 7, no. 7, p. eabc8843, 2021.

[5] G. L. Villanueva, G. Liuzzi, S. W. Aoki, Shohei adn Stone, A. Brines, I. R. Thomas, M. A. Lopez-Valverde, L. Trompet, E. Justin, F. Daerden, *et al.*, "The deuterium isotopic ratio of water released from the Martian caps as measured with TGO/NOMAD," 2022. unpublished.

[6] M. Chaffin, J. Deighan, N. Schneider, and A. Stewart, "Elevated atmospheric escape of atomic hydrogen from mars induced by high-altitude water," *Nature geoscience*, vol. 10, no. 3, pp. 174–178, 2017.

[7] A. C. Vandaele, E. Neefs, R. Drummond, I. R. Thomas, F. Daerden, J.-J. Lopez-Moreno, J. Rodriguez, M. R. Patel, G. Bellucci, M. Allen, *et al.*, "Science objectives and performances of NOMAD, a spectrometer suite for the ExoMars TGO mission," *Planetary and Space Science*, vol. 119, pp. 233–249, 2015.

[8] A. C. Vandaele, J.-J. Lopez-Moreno, M. R. Patel, G. Bellucci, F. Daerden, B. Ristic, S. Robert, I. Thomas, V. Wilquet, M. Allen, *et al.*, "NOMAD, an integrated suite of three spectrometers for the ExoMars trace gas mission: Technical description, science objectives and expected performance," *Space Science Reviews*, vol. 214, no. 5, pp. 1–47, 2018.

[9] M. A. Lopez-Valverde, B. Funke, A. Brines, A. Stolzenbach, A. Modak, F. Gonzalez-Galindo, *et al.*, "Martian atmospheric temperature and density profiles during the 1st year of NOMAD/TGO solar occultation measurements," 2022. unpublished.

[10] G. P. Stiller, "The Karlsruhe Optimized and Precise Radiative transfer Algorithm (kopra)," -, 2000.

[11] F. Forget, F. Hourdin, R. Fournier, C. Hourdin, O. Talagrand, M. Collins, S. R. Lewis, P. L. Read, and J.-P. Huot, "Improved general circulation models of the Martian atmosphere from the surface to above 80 km," *Journal of Geophysical Research: Planets*, vol. 104, no. E10, pp. 24155–24175, 1999.

[12] D. M. Murphy and T. Koop, "Review of the vapour pressures of ice and supercooled water for atmospheric applications," *Quarterly Journal of the Royal Meteorological Society: A journal of the atmospheric sciences, applied meteorology and physical oceanography*, vol. 131, no. 608, pp. 1539–1565, 2005.

[13] A. Stolzenbach, M. A. Lopez-Valverde, B. Funke, A. Brines, A. Modak, F. Gonzalez-Galindo, *et al.*, "Martian atmospheric aerosols composition and distribution retrievals during the 1st martian year of NOMAD/TGO solar occultation measurements," 2022. unpublished.

[14] S. Aoki, A. C. Vandaele, F. Daerden, G. L. Villanueva, G. Liuzzi, Clancy, M. A. Lopez-Valverde, A. Brines, I. Thomas, L. Trompet, J. Erwin, *et al.*, "Global vertical distribution of water vapor on Mars: Results from 3.5 years of ExoMars-TGO/NOMAD science operations," 2022. unpublished.